Structure-Property Correlation for Nitride Superconductors for Use in Ultra Low Energy Applications

Jana Alomairi, Niladri Banerjee

Jana.alomair26@kaust.edu.sa, N.Banerjee@imperial.ac.uk

Abstract

Niobium nitride (NbN) is a strongly-coupled s-wave superconductor central to many technologies where a high and reproducible transition temperature (T_c) is essential. Prior work showed that T_c in pulsed-laser-deposited δ NbNcan be tuned through nitrogen partial pressure via lattice-strain and carrier-density effects, but did not analyse normal-state resistivity directly as a predictor of T_c. Here we combine published transport data for epitaxial NbN films grown on MgO(001) at 0–70 mTorr with atomic force microscopy performed in this work (32 scans, 3–4 positions per film, analysed in Gwyddion). Resistivity correlates strongly with T_c (r = 0.88), comparable to the lattice parameter (r = +0.96), while surface roughness shows no significant relationship with either. Resistivity varies parabolically with pressure (R^2 = 0.98) falling with pressure below 25 mTorr and rising above 30 mTorr., independently reproducing the growth mode crossover previously observed in X-ray diffraction. Comparison with seven thicker reactively sputtered NbN films reveals the same qualitative trend (r = 0.96 against ln ρ) but an offset ranging between 3–6K at matched resistivity, indicating that resistivity-based T_c calibration is deposition-technique specific.

Date: August 24, 2026

Contents

1 Introduction **2**

2 Related Work **3**

3 Methodology **4**

3.1 Method details 4

3.2 Evaluation Procedure 5

4 Results **6**

4.1 Baseline 6

4.2 Predictors of T_c 6

4.3 Pressure dependence of resistivity 7

4.4 Surface morphology results 8

4.5 Cross-technique comparison 9

4.6 Threshold dependence of droplet metrics 9

5 Discussion **9**

6 Limitations and Future Work **10**

7 Conclusion **11**

8 References **11**

1 Introduction

Superconductivity is a quantum state of matter that has a mixture of electric and magnetic properties which appears in certain metals when cooled cryogenically [3]. It is characterized by two defining macroscopic phenomena: the total disappearance of electrical resistance (R) below a critical transition temperature (T_c) and perfect diamagnetism, known as the Meissner–Ochsenfeld effect, where the interior magnetic flux is actively expelled (B = 0). At the microscopic level, the Bardeen–Cooper–Schrieffer (BCS) theory demonstrates that an attractive interaction mediated by lattice vibrations (phonons) causes conductive electrons near the Fermi level to bond into Cooper pairs [3]. In strongly coupled superconductors such as niobium nitride (NbN), this electron–phonon interaction strength ($\lambda_{\text{el-ph}}$) directly links the macroscopic transition temperature to structural and electronic parameters: McMillan theory specifically links the electronic density of states at the Fermi level N(0) with T_c, and Allen–Dynes theory links the lattice parameters to the change in T_c. [1]

Niobium nitride (NbN) was chosen as a sample in many researches [1][2][4] because it has a number of interesting properties, such as chemical inertness, high hardness and relatively high superconductivity transition temperature (17.3 K) compared to other metals [1][2]. NbN is a strongly coupled, s-wave superconductor [1][2], essiential to a range of quantum and cryogenic technologies, including superconducting quantum computing [5]. NbN is the leading material for superconducting nanowire single-photon detectors, which are widely applied in quantum key distribution and optical quantum computation [6], as well as kinetic-inductance resonators and terahertz hot-electron bolometers [1]. All of these devices depend sensitively on achieving a high, reproducible transition temperature (T_c), since higher T_c permits operation at more accessible cryogenic temperatures and improves device stability.

NbN films are grown mainly by two deposition techniques: reactive sputtering and pulsed laser deposition (PLD). A previous study [1] used PLD because it enables epitaxial growth with precise control of δ-NbN stoichiometry and compatibility with magnetic heterostructures, allowing the structural and electronic factors governing T_c to be isolated. Whether the same relationships hold for films grown by reactive sputtering [2] (the more conventional technique) remains unresolved, yet is essential knowledge for reliably engineering NbN based devices.

Prior work [1] demonstrated that in PLD grown epitaxial NbN films, T_c varies non monotonically with nitrogen partial pressure during growth (figure no.), and that this variation is well explained by combined changes in lattice strain and electronic density of states at the Fermi level, using the McMillan and Allen–Dynes strong-coupling framework. Notably, that study found no explicit correlation between disorder (quantified via residual resistivity ratio, RRR) and T_c, suggesting that disorder-related scattering does not dominate the observed T_c trend. Normal-state resistivity itself, however, was not analysed directly as a predictor of T_c. Two open questions therefore remain.

1. First, it is unclear whether surface characteristics of the films (roughness and droplet morphology) which vary across growth conditions and across a single sample, influence the relationship between normal state resistivity and T_c, a factor not explicitly addressed in the existing structural framework.
2. Second, it is resolved whether the pressure dependent relationship between resistivity and T_c observed in PLD grown NbN matches the trends long reported for reactively sputtered NbN, the more conventional and widely used deposition technique, where T_c is also known to depend primerly on carrier concentration [2].

This study assumes the films retain the cubic rock-salt δ-NbN phase across the pressure

range, consistent with the XRD characterization reported for the parent sample set [1]. Transport parameters (T_c, ΔT_c, RRR, lattice parameter, thickness and resistivity) are taken from that study, where T_c was defined at (50% of the normal-state resistance; all surface characterization and statistical analysis reported here were performed in this work. Atomic force microscopy (AFM) scans are limited to 3–4 positions per film, and because RMS roughness is scan-size dependent, our values are not directly comparable to those measured over different areas. Droplet metrics depend on the height threshold used for grain detection: measured droplet height correlates with the threshold at r = 0.999 and is therefore excluded from interpretation, while radius, density and grain count show no significant threshold dependence ($|r| < 0.30$) after averaging over 3–4 positions per film. Droplets are nonetheless spatially non-uniform, mean radius varies by up to 27 nm between positions within a single film, comparable to the 15 nm variation observed across the full pressure range, so the radius–pressure trend should be regarded as indicative rather than firmly established. Finally, the comparison with sputtered NbN rests on literature values rather than a controlled side-by-side study, and is limited by film thickness (20–28 nm for PLD films versus >50 nm in the sputtering reference [2]) and by differing T_c criteria (50% versus 10%), though the latter works against the observed offset rather than producing it.

To address these questions, we characterize a series of epitaxial NbN thin films grown on MgO (001) substrates by PLD across a range of nitrogen partial pressures (0–70 mTorr), combining the 32 AFM scans (3–4 positions per film, analysed in Gwyddion to extract surface roughness, droplet radius and droplet density) with published transport data [1] for T_c, ΔT_c, RRR, and normal-state resistivity. By correlating resistivity against T_c alongside surface characteristic data for each sample, quantified using Pearson and Spearman coefficients with significance testing, we assess whether surface morphology modifies or explains variation in the resistivity–T_c relationship beyond what is captured by lattice parameter and carrier density alone. By separately fitting resistivity and T_c against nitrogen growth pressure and comparing the resulting trends to those reported for reactively sputtered NbN films [2], we test whether the underlying structure property relationship in NbN is a general feature of the material system or specific to the PLD growth mechanism. Together, these two comparisons extend the existing structural framework for T_c control in NbN and clarify the role of both surface morphology and deposition technique in determining superconducting performance.

2 Related Work

Reactive magnetron sputtering has historically been the dominant method for growing NbN thin films, with reported T_c ranging from 9.99 to 16.11 K depending sensitively on carrier concentration [2]. In sputtering, reactive nitrogen participates directly in compound formation, so growth parameters modify stoichiometry as an inherent part of the process, a mechanism Chockalingam et al. used in his research, varying sputtering power and N_2/Ar ratio to tune carrier density [2]. Pulsed laser deposition (PLD) instead largely preserves target stoichiometry and allows growth on magnetic underlayers [1], at the cost of ejecting micron-scale droplets onto the film surface, a characteristic intrinsic to laser ablation [1][4].

Early PLD work by Treece et al. [7] showed that T_c depends strongly on substrate: epitaxial films on MgO(100) reached 16.1 K at 60 μΩ·cm while polycrystalline films grown simultaneously on fused silica reached only 11.8 K at 120 μΩ·cm, attributed to grain-boundary scattering. This established a resistivity–T_c link, but only for two samples. Farha et al. [4] varied laser fluence, nitrogen pressure and substrate temperature systematically, reporting T_c from 7.66 to 15.07 K and measuring RMS roughness by AFM over 2 × 2 μm areas which is the closest prior work to our surface analysis, though their films were multi phase mixtures of δ-NbN and β-Nb_2N, so T_c

variation was dominated by phase composition rather than continuous structural tuning. Li et al. [1] removed this confound by depositing from a stoichiometric target with nitrogen acting as an inert ballast gas, holding the δ-NbN phase fixed while producing an 8 K non monotonic T_c variation, and found that T_c correlates with lattice parameter and density of states N(0) but shows no explicit trend with residual resistivity ratio (RRR).

Our study inherits the main advantage of that sample set, a fixed δ-NbN phase across all pressures, so T_c variation reflects continuous structural change rather than phase transitions. The trade-offs are film thickness (19.95–27.86 nm here versus films exceeding 50 nm in the sputtering comparison [2], chosen there to avoid epitaxial strain effects) and AFM scan size (18-20 µm here versus the 2 × 2 µm scans of Farha et al. [4]), the latter improving droplet statistics but making RMS values non-comparable across studies.

Three gaps remain. First, no prior PLD study has examined normal-state resistivity directly as a predictor of T_c: Treece et al. [7] reported it for two films, and Li et al. [1] used RRR only as a negative control. Second, no study has tested whether surface morphology modifies the resistivity–T_c relationship, despite droplets being unavoidable in PLD [1][4]. Third, the two literatures appear to disagree on mechanism: Chockalingam et al. [2] report no correlation between T_c and lattice parameter in sputtered films, whereas Li et al. [1] find lattice parameter to be the dominant structural predictor, but no direct comparison has been made. This work addresses all three: quantifying the resistivity–T_c correlation across nine growth pressures, testing whether AFM derived surface parameters correlate with either quantity, and comparing our fitted relationship against published sputtered NbN values at matched resistivity.

3 Methodology

3.1 Method details

Transport measurements were performed by Li et al. [1]; AFM characterisation and all statistical analysis presented here are original to this work. Our method combines these two datasets across a shared set of NbN thin films, so that morphological and superconducting properties can be correlated per sample. as seen in figure (1) The films are epitaxial NbN grown on MgO (001) by PLD at nine nitrogen partial pressures. For each sample, (i) AFM imaging at 3–4 positions characterises surface morphology and spatial uniformity, and (ii) transport parameters: T_c, ΔT_c, RRR, normal-state resistivity, lattice parameters and thickness are taken from the Physical Properties Measurment System (ppms) measurements reported in [1]. The two datasets are merged at sample level, analysed for correlation, and compared against published values for reactively sputtered NbN [2].

Steps of our system:.

1. **Sample set.** NbN thin films grown by PLD from a stoichiometric NbN target onto MgO(001) substrates at nitrogen partial pressures of 0, 10, 15, 25, 30, 40, 50, 60 and 70 mTorr [1].
2. **AFM imaging.** Each film imaged at 3–4 fixed positions (corners and centre), giving 32 scans in total.
3. **Image processing.** Each scan was levelled and zeroed using Gwyddion software, then a threshold was set to identify droplets, from which morphological parameters are extracted and averaged across positions.
4. **Transport characterisation.** Transport parameters taken from Li et al. [1], where resistance was measured as a function of temperature and T_c extracted at 50% of the 20K normal-state resistance, ΔT_c as the transition width, RRR as R(270 K)R(20 K), and normal-state resistivity

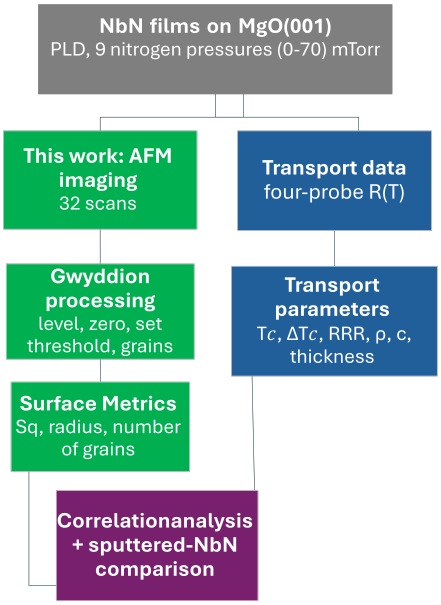


Figure 1 method framework

ρ extracted from the measured resistance R in the normal metallic state (T > T_c).

5. **Correlation analysis.** Per sample values combined; Pearson and Spearman correlations computed between all pairs, with functional fits against growth pressure.
6. **Cross-technique comparison.** An empirical fit of T_c against ln(ρ) for the PLD films was evaluated at the resistivities of published sputtered NbN films [2], and the difference between predicted and measured T_c used to quantify the offset between techniques.

3.2 Evaluation Procedure

AFM images were processed in Gwyddion 2.61 (levelling, height thresholding, grain detection, and extraction of roughness and droplet statistics); all subsequent analysis was carried out in Microsoft Excel. The dataset combines transport parameters for nine films spanning 0–70 mTorr, taken from Li et al. [1], with 32 AFM scans acquired in this work at 3–4 positions per film, yielding RMS roughness, mean droplet radius and grain count; per-sample values are means across positions, with standard deviations retained as a measure of a single films variability. Published resistivity and T_c values for sputtered [2] and earlier PLD-grown [7] NbN were taken from the literature for cross-technique comparison. Relationships were quantified by the Pearson coefficient r, with two-tailed p-values from $t = r\sqrt{(n-2)/(1-r^2)}$ and $p < 0.05$ as the significance threshold, corresponding to $|r| > 0.67$ for nine samples. The lattice parameter–T_c correlation was computed first as a consistency check against [1] and used as the baseline for judging the predictive power of resistivity. Pressure dependence was assessed by comparing R^2 for linear and quadratic fits and by splitting the set into low and high-pressure regimes. Because droplet height is measured relative to the detection threshold, and thresholds varied between scans, droplet height was excluded from interpretation.

4 Results

4.1 Baseline

Two baselines are used. The first is physical: Li et al. [1] identify the out-of-plane lattice parameter as the dominant structural predictor of T_c in these films, so the correlation between lattice parameter and T_c sets the standard against which the predictive power of resistivity is judged. The second is statistical: with nine samples, a correlation must exceed $|r| = 0.67$ to reach $p < 0.05$, so any parameter falling below this cannot be distinguished from chance.

Worth noting that correlation coefficients alone are not treated as sufficient evidence of a relationship. Each significant correlation was inspected graphically, and results showing a statistical association without a visible trend or a plausible physical mechanism are reported as such rather than interpreted as findings.

4.2 Predictors of T_c

Parameter	Source	r	p	R^2	Does it Meet Baseline
Lattice paramete c (baseline)	[1]	+0.955	0.0001	0.91	_
ln (resistivety)	[1]	-0.921	0.0004	0.85	yes
Resistivity	[1]	-0.883	0.0016	0.78	yes
RRR	[1]	+0.736	0.024	0.54	see text
Surface roughness (Sq)	this work	-0.32	0.40	0.10	no
Film thickness	[1]	-0.016	0.97	0.00	no

Table 1 **Table 1.** Correlation of each measured parameter with T_c across nine growth pressures. Baseline is the lattice-parameter correlation, which quantifies the quasi-linear trend reported by Li et al. [1]; the significance threshold for $n = 9$ is $|r| = 0.67$.

Resistivity correlates with T_c (Table 1) at $r = 0.883$ across a resistivity range of 117.5–496.1 μΩ·cm and a T_c range of 3.02–12.45 K, rising to $r = 0.921$ against ln . This approaches the lattice-parameter baseline, explaining 78–85% of the variance in T_c against the baseline's 91%. Neither surface roughness nor film thickness reaches the detection threshold.

RRR returns a nominally significant coefficient ($r = +0.736$, $p = 0.024$), but the corresponding plot shows no clear trend: the film grown at 0 mTorr has the third-highest RRR in the set yet a T_c of only 7.37 K, while the film at 25 mTorr combines a low RRR of 0.631 with a T_c of 11.86 K. This is consistent with Li et al. [1], who report no explicit correlation between RRR and T_c. The coefficient is therefore reported for completeness but not interpreted as a physical relationship.

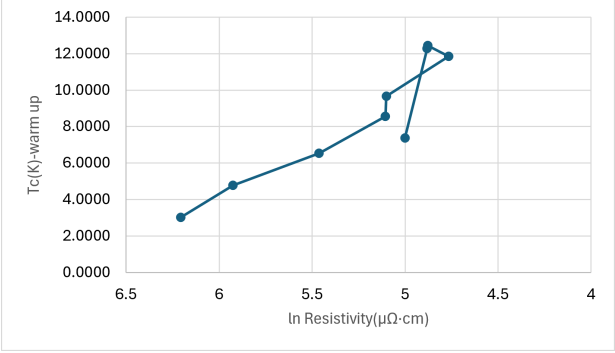


Figure 2 T_c against normal-state resistivity, with fitted trendline.

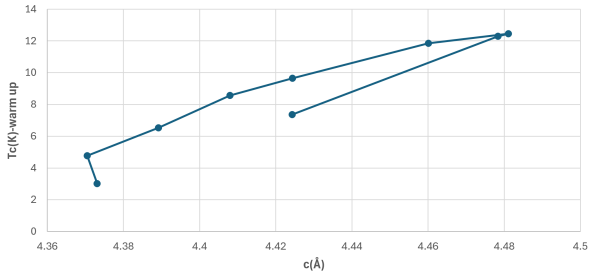


Figure 3 T_c against out-of-plane lattice parameter, shown as the baseline comparison.

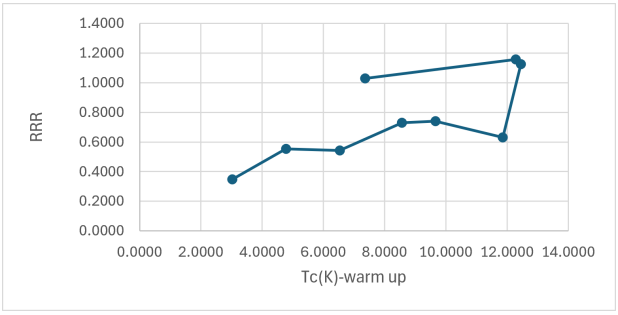


Figure 4 T_c against RRR, showing the absence of a visible trend despite a significant coefficient.

4.3 Pressure dependence of resistivity

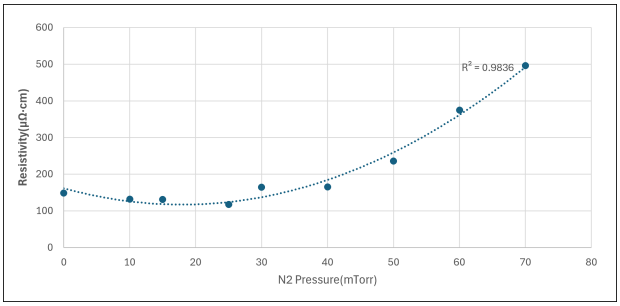


Figure 5 Normal-state resistivity as a function of nitrogen partial pressure for the nine PLD-grown NbN films. Markers are measured values; the curve is a least-squares quadratic fit ($R^2 = 0.984$), which describes the data far better than a straight line ($R^2 = 0.737$). The fitted minimum falls at 17.9 mTorr, between the 15 and 25 mTorr films, so its position is interpolated rather than measured. Resistivity decreases with pressure below 25 mTorr and increases above 30 mTorr, reproducing in transport the crossover from dense to porous columnar growth that Li et al. [1] infer from lattice-parameter evolution.

Parameter	R^2 linear	R^2 quadratic	Turning point
Resistivity [1]	0.737	**0.984**	minimum at 17.9 mTorr
T_c [1]	0.583	0.831	maximum at 19.9 mTorr

Table 2 Functional form of the pressure dependence. Resistivity varies with pressure at $r = +0.858$ ($p = 0.003$), but a quadratic fit describes it far better than a straight line ($R^2 = 0.984$ versus 0.737), with a minimum at 17.9 mTorr which makes it within 2 mTorr of the T_c maximum.

Parameter	0–25 mTorr	30–70 mTorr
Resistivity vs pressure	$r = 0.982$ ($p = 0.018$)	$r = +0.953$ ($p = 0.012$)
T_c vs pressure	$r = +0.746$ ($p = 0.254$)	$r = 0.997$ ($p = 0.0004$)

Table 3 Regime-split analysis, dividing the sample set at 30 mTorr.

Resistivity reverses sign across the two regimes, falling significantly with pressure below 25 mTorr and rising significantly above 30 mTorr. Li et al. [1] infer a crossover from dense to porous columnar growth over this pressure range from XRD and lattice-parameter evolution; the resistivity data reproduces that crossover independently, and with a better-defined turning point than the structural data.

4.4 Surface morphology results

Parameter	vs pressure	vs resistivity
Mean droplet radius	$r = +0.680$ ($p = 0.044$)	$r = +0.529$ ($p = 0.144$)
Grain count	$r = 0.584$ ($p = 0.099$)	$r = 0.792$ ($p = 0.011$)
RMS roughness (Sq)	$r = +0.588$ ($p = 0.096$)	$r = +0.389$ ($p = 0.300$)

Table 4 AFM-derived parameters versus growth pressure and resistivity ($n = 9$, this work).

Mean droplet radius increases from 64.7 nm at 10 mTorr to 79.9 nm at 70 mTorr, correlating with pressure at $r = +0.680$, clearing the significance threshold by a narrow margin. The trend is not monotonic (radius decreases at 10, 40 and 60 mTorr) and the scatter between measurement positions within a single film is comparable to the variation between films, so this result is treated as indicative rather than established.

Grain count correlates with resistivity at $r = 0.792$, with the two highest-resistivity films (60 and 70 mTorr) showing 592 and 677 grains against 800–890 for the remainder. Grain count and droplet radius are themselves related ($r = 0.71$), larger droplets accompanying fewer detected grains. Surface roughness shows no significant relationship with pressure, resistivity or T_c; Farha et al. [4] likewise report non-monotonic roughness behaviour in PLD-grown NbN_x.

4.5 Cross-technique comparison

Source	Technique	(μ·cm)	Measured T_c (K)	Predicted T_c (K)	Difference
Chockalingam et al. [2]	sputtered	94.6	16.11	12.89	+3.22
Chockalingam et al. [2]	sputtered	147.9	15.14	10.13	+5.01
Chockalingam et al. [2]	sputtered	189.1	13.57	8.60	+4.97
Chockalingam et al. [2]	sputtered	194.0	12.24	8.45	+3.79
Chockalingam et al. [2]	sputtered	225.7	11.61	7.51	+4.10
Chockalingam et al. [2]	sputtered	312.0	11.27	5.50	+5.77
Chockalingam et al. [2]	sputtered	383.1	9.99	4.23	+5.76
Treece et al. [7]	PLD	60	16.1	15.71	+0.39
Treece et al. [7]	PLD	120	11.8	11.42	+0.38

Table 5 Measured T_c for reactively sputtered NbN [2] compared against the value predicted by the fitted PLD relationship, T_c = 6.19 ln() + 41.05. Independently grown PLD films [7] are included as a within-technique control.

Sputtered films show the same qualitative relationship (r = 0.96 against $ln\rho$, n = 7) but sit systematically above the PLD trend, by 3.22 to 5.77 K. Independently grown PLD films [7] fall within 0.4 K of the same fit. Fitted slopes are 6.19 K per e-fold in ρ for the PLD films against 4.55 K for the sputtered films.

A further difference emerges in which parameter predicts T_c. Lattice parameter correlates with T_c at r = +0.955 in the PLD films [1] but at r = 0.33 (p = 0.46) in the sputtered films [2]; conversely, the density of states at the Fermi level correlates with T_c at r = +0.962 in the sputtered films [2].

4.6 Threshold dependence of droplet metrics

Droplet height is measured by Gwyddion relative to the detection threshold, and thresholds varied between scans. Measured droplet height therefore reflects the threshold rather than the film, and is excluded from interpretation. Radius, density and grain count are measured from the projected extent of marked regions and are correspondingly less sensitive to threshold placement; these are retained.

5 Discussion

The central result of Section 4.2 is resistivity predicting T_c at r = 0.88 against the lattice-parameter baseline of +0.96 which is not obvious given that Li et al. [1] found no RRR–T_c trend. The resolution is that RRR is a ratio, and normalising by low-temperature resistivity discards the absolute magnitude of scattering that resistivity retains. The correlation doesn't imply causation: both quantities depend on carrier density, which raises T_c through electron–phonon coupling while lowering resistivity, so the two likely respond to a shared underlying variable. That RRR shows a significant coefficient but no visible trend illustrates why coefficients alone are insufficient evidence.

The null result on surface characteristics met expectations, since superconductivity is a bulk property while roughness and droplets describe the outer boundary. It eliminates a plausible alternative explanation, though with nine samples it should be read as a failure to detect rather than a demonstration of absence.

The most unexpected finding is in Section 4.3: resistivity follows a quadratic pressure dependence with $R^2 = 0.984$ which makes a better fit than T_c achieves, and reverses sign near 30 mTorr. This reproduces, in an independent measurement channel, the crossover from dense to porous columnar growth that Li et al. [1] infer from XRD. Porous growth introduces voids and grain boundaries that scatter carriers, exactly as the rise in resistivity predicts. The near coincidence of turning points (17.9 versus 19.9 mTorr) supports a common origin; that they differ slightly indicates resistivity is not a perfect proxy near the optimum.

Section 4.4 shows droplet radius increasing with pressure, consistent with gas-phase scattering removing small particulates. Grain count correlates with resistivity in the opposite sense to droplet-induced scattering, ruling out droplets as a cause and pointing to both being consequences of the same growth-mode transition.

The cross-technique comparison met expectations qualitatively but not quantitatively. Both techniques show higher resistivity accompanying lower T_c, confirming this as a property of NbN. The 3–6 K offset, with independent PLD films [7] falling within 0.4 K of our fit, suggests genuine technique dependence, plausibly from PLD-induced strain suppressing T_c without a proportional resistivity increase. Most strikingly, lattice parameter predicts T_c in PLD films ($r = +0.96$) but not sputtered ones ($r = 0.33$), where density of states does instead ($r = +0.96$), indicating different dominant mechanisms rather than different film quality. This is qualified by the thickness difference between datasets, which our data cannot resolve.

6 Limitations and Future Work

Sample size. With nine films, correlations below $|r| = 0.67$ are undetectable, so the roughness and thickness nulls show a failure to detect rather than an absence of relationship, and the droplet radius result clears the threshold only narrowly. Next step: extend the pressure series, particularly between 15 and 30 mTorr.

Droplet analysis. Thresholds were set per scan rather than by a single rule, so droplet dimensions are not strictly comparable and droplet height had to be excluded; droplets are also spatially non-uniform, with within film scatter comparable to between film variations. Next step: reprocess all scans at one absolute threshold defined from the background roughness, and increase to eight or more positions per film.

Roughness comparability. RMS roughness is scan-size dependent, so our (18-20 μm) values are not comparable with the 2 μm scans used elsewhere [4] and do not track those reported for the same films in [1]. Next step: acquire matched scans at both sizes and confirm the scan area used in the parent study.

Cross-technique comparison. The comparison with sputtered NbN [2] uses published values rather than side-by-side growth, and is confounded by thickness (19.95–27.86 nm versus >50 nm) and differing T_c criteria (50% versus 10%). Next step: grow a PLD thickness series spanning 20–80 nm at fixed pressure to test whether the offset survives thickness matching.

All transport data comes from a single chamber and substrate [1], so the fitted relationship may not generalise. Next step: repeat the analysis on films from an independent PLD system.

Extensions. That lattice parameter predicts T_c in PLD films but not sputtered ones where density of states does instead, suggests different dominant mechanisms, testable by combining Hall effect and XRD measurements on thickness matched films from both techniques. Practically, any resistivity based screening calibration should be established at device relevant thicknesses, often below 10 nm, where finite-size effects are strongest.

7 Conclusion

This project tested whether normal-state resistivity predicts the superconducting transition temperature of PLD-grown -NbN. Combining 32 AFM scans acquired in this work with published transport data for nine films spanning 0–70 mTorr [1], we find resistivity correlates with T_c at r = 0.88, explaining 78–85% of the variance against the 91% explained by the lattice parameter (the parameter previously identified as dominant) while requiring only a standard cooldown rather than X-ray diffraction. Surface roughness, thickness and droplet morphology show no significant relationship with T_c, confirming that the variation is intrinsic. Resistivity also varies parabolically with pressure ($R^2 = 0.98$) and reverses sign near 30 mTorr, independently reproducing the growth-mode crossover previously inferred from X-ray diffraction. Comparison with seven sputtered films [2] shows the same qualitative trend but a 3–6 K offset, and lattice parameter predicts T_c in PLD films (r = +0.96) but not sputtered ones (r = 0.33), where density of states does instead, indicating different dominant mechanisms rather than different quality. The main takeaway is that normal-state resistivity is a fast, non-destructive substitute for structural characterisation when predicting T_c in NbN, but the calibration is specific to the deposition technique and cannot be transferred between them.

8 References

[1] Li Z, Johnson F, Mondal P, Rodriguez-Kazeem W, Cohen L, Banerjee N. Dependence of the superconducting transition temperature on the electronic density of states and lattice parameter in pulsed laser deposited niobium nitride thin films. *Superconductor Science and Technology* 2026;**39**:055007. DOI: 10.1088/1361-6668/ae61fe

[2] Chockalingam SP, Chand M, Jesudasan J, Tripathi V, Raychaudhuri P. Superconducting properties and Hall effect of epitaxial NbN thin films. *Physical Review B* 2008;**77**:214503. DOI: 10.1103/PhysRevB.77.214503

[3] Rose-Innes AC, Rhoderick EH. *Introduction to Superconductivity*. 2nd ed. Oxford: Pergamon Press; 1978.

[4] Farha AH, Ufuktepe Y, Myneni G, Elsayed-Ali HE. Pulsed laser deposition of niobium nitride thin films. *AIP Conference Proceedings* 2015;**1687**:020003. DOI: 10.1063/1.4935317

[5] Kim S, Terai H, Yamashita T, Qiu W, Fuse T, Yoshihara F, Ashhab S, Inomata K, Semba K. Enhanced coherence of all-nitride superconducting qubits epitaxially grown on silicon substrate. *Communications Materials* 2021;**2**:98.

[6] You L. Superconducting nanowire single-photon detectors for quantum information. *Nanophotonics* 2020;**9**:2673–92.

[7] Treece RE, Horwitz JS, Claassen JH, Chrisey DB. Pulsed laser deposition of high-quality NbN thin films. *Applied Physics Letters* 1994;**65**:2860–2. DOI: 10.1063/1.112516